

# Thresholds for post-selected quantum error correction from statistical mechanics

Lucas H. English,<sup>\*</sup> Dominic J. Williamson,<sup>†</sup> and Stephen D. Bartlett  
*School of Physics, University of Sydney, Sydney, New South Wales 2006, Australia*  
 (Dated: October 29, 2024)

We identify regimes where post-selection can be used scalably in quantum error correction (QEC) to improve performance. We use statistical mechanical models to analytically quantify the performance and thresholds of post-selected QEC, with a focus on the surface code. Based on the non-equilibrium magnetization of these models, we identify a simple heuristic technique for post-selection that does not require a decoder. Along with performance gains, this heuristic allows us to derive analytic expressions for post-selected conditional logical thresholds and abort thresholds of surface codes. We find that such post-selected QEC is characterised by four distinct thermodynamic phases, and detail the implications of this phase space for practical, scalable quantum computation.

*Introduction.*—Quantum computers are expected to solve certain problems that are intractable with conventional methods [1, 2]. However, quantum information is easily corrupted by interactions with the environment, and current qubit and gate error rates are too high to allow for large-scale quantum computations without some means to correct these errors [3]. By using quantum error correcting codes and the techniques of fault-tolerant quantum computing, large-scale quantum computations with arbitrary accuracy are predicted to be possible [4, 5]. The overheads needed for quantum error correction, in terms of qubit redundancy and additional circuit complexity, can be very large, and there is a need for new approaches to reduce these overheads in practice [6–8].

Post-selection has been proposed as a means to enhance the performance of quantum error correction by aborting, and potentially reinitializing, an experiment if the success of correction is sufficiently uncertain [9–14]. Knill first proposed such an enhancement in Ref. [15], demonstrating improved threshold estimates for concatenated distance-2 codes and posing the question: *are thresholds of post-selected computing strictly higher than those of standard quantum computing?* Recently, numerical and experimental results have demonstrated improved conditional logical error rates from post-selection [16–22]. Despite these promising results, the theoretical limits of performance gains enabled by post-selected QEC are poorly understood.

Models from statistical mechanics provide a powerful set of tools for quantifying these limits. For a QEC code, the value of the threshold with optimal decoding can be reformulated as the location of a phase transition in a statistical mechanical model [23]. This formulation was originally proposed for the surface code [23] and was later generalized to arbitrary stabilizer codes [24]. Recently, this approach has been extended to connect the stability of topologically-ordered phases under local perturbations with the thresholds of topological quantum error correcting codes [25].

In this work, we modify the mapping from Pauli stabilizer codes to disordered statistical mechanical models to include the effects of post-selection on quantum

error correction. With this mapping, we demonstrate that optimal post-selection can be performed by setting a minimum cutoff value for the largest disordered partition function representing a logical coset probability using a maximum-likelihood decoder (MLD). Based on this connection with statistical mechanical models, we propose a simple heuristic post-selection rule that does not require any decoding prior to aborting, and analytically compute bounds on its conditional logical thresholds. We apply a mean-field argument to analytically determine the abort threshold of the heuristic post-selection rule. We identify four distinct thermodynamic phases for post-selected quantum error correction, and identify regimes where post-selection can be advantageous in scalable fault-tolerant quantum computing. Finally, we apply the heuristic post-selection rule to experimental data taken from a recent QEC demonstration by Google [26].

*Statistical mechanical mapping.*—Pauli stabilizer codes can be mapped to a Hamiltonian, in which the stabilizer measurement outcomes correspond to classical spin degrees of freedom [23], and where physical Pauli errors  $E \in \mathcal{P}^{\otimes n}$  are mapped to quenched disorder parameters. We parameterize the Hamiltonian  $H_E$  by the time-independent random variable  $E$ . We associate a classical spin degree of freedom  $s_k = \pm 1$  to represent the possible measurement outcomes of each stabilizer  $S_k$ . The classical spin Hamiltonian produced by the statistical mechanical mapping can be written

$$H_E(\vec{s}) = - \sum_{i, \sigma \in \mathcal{P}_i} \overbrace{J_i(\sigma)}^{\text{Strength}} \overbrace{[\sigma, E]}^{\text{Disorder}} \overbrace{\prod_{k: [\sigma, S_k] = -1}}^{\text{Interactions}} s_k, \quad (1)$$

where  $[\cdot, \cdot]$  is the scalar commutator defined by  $AB = [A, B]BA$ ,  $\mathcal{P}_i$  is the local Pauli group on qubit  $i$ ,  $J_i(\sigma)$  are the interaction strengths in the model which are determined by the underlying noise process, and  $[\sigma, E]$  is the disorder in the system [24]. Given  $E \in \mathcal{P}^{\otimes n}$  and  $\sigma \in \mathcal{P}_i$ , we have  $[\sigma, E] = \pm 1$  corresponding to ferromagnetic and antiferromagnetic couplings, respectively.

One can compute the phase diagram by fixing a Pauli noise process, that is, a probability distribution  $\mathbb{P}(E)$ . The phase transition from an ordered to a disordered

phase occurs when the quenched average free energy  $[\langle F \rangle_{Z[E]}]_E$  becomes non-analytic. We follow the notation used in Ref. [25], where  $\langle \cdot \rangle_{Z[E]}$  denotes the thermal average of a thermodynamic quantity with disordered partition function  $Z[E]$ , and  $[\cdot]_E$  denotes the quenched average over disorder parameters  $E$ . Assuming independent single-qubit Pauli noise, the Nishimori conditions are said to hold with respect to the noise distributions  $\{\mathbb{P}_i(\sigma)\}_i$  if

$$\beta J_i(\sigma) = \frac{1}{|\mathcal{P}|} \sum_{\tau \in \mathcal{P}_i} \log \mathbb{P}_i(\tau) [\![\sigma, \tau^{-1}]\!], \quad (2)$$

for all qubits  $i$  and Paulis  $\sigma \in \mathcal{P}_i$  [24]. The Nishimori conditions define a manifold on the state space of the system in which a local  $\mathbb{Z}_2$  gauge symmetry acts. This gauge symmetry leads to identities relating thermodynamic quantities, including the internal energy of a random-bond Ising model [27]. Under the Hamiltonian in Eq. (1), along the Nishimori line, the phase transition of the statistical mechanical model corresponds to the logical threshold of the code under maximum-likelihood decoding [24]. Moreover, the Hamiltonian satisfies the symmetry  $H_{E S_k}(\vec{s}) = H_E(\vec{s} + \hat{k})$ . Together, these properties imply that the disordered partition function on the Nishimori line encodes an error's logical coset probability  $Z_E = \sum_{\vec{s}} e^{-\beta H_E(\vec{s})} = \sum_{S \in \mathcal{S}} e^{-\beta H_{ES}(\vec{0})} = \mathbb{P}(\bar{E})$ .

For example, the toric code under an independent depolarizing noise channel is represented by a disordered eight-vertex model [24]. Similarly, the toric code under an independent bit-flip noise channel is represented by a random-bond Ising model [23].

Post-selection partitions the total set of syndromes into an accept and an abort partition. However, as the classical spin Hamiltonian is parametrized by the Pauli error acting on the code, we instead treat post-selection as partitioning the total set of errors  $\mathcal{E} \in \mathcal{P}^{\otimes n}$  into an accept and an abort partition,  $\mathcal{E} = \mathcal{E}_{\text{accept}} \cup \mathcal{E}_{\text{abort}}$ . By constraining errors which produce equivalent syndromes to lie in the same partition, we induce a canonical isomorphism between the partition of errors and syndromes. Under the statistical mechanical mapping, the code's conditional logical threshold after post-selection can be determined by taking the quenched average over only the accepted set  $\mathcal{E}_{\text{accept}}$ .

We define a post-selection rule  $R$  by mapping a post-selection parameter  $c \in [0, 1]$  to the abort partition of errors,  $R(c) = \mathcal{E}_{\text{abort}}$ . Here, we set the convention that  $|R(c)|$  is nondecreasing with  $c$ ,  $R(0) = \emptyset$ , and  $R(1) = \mathcal{E}$  is the maximal set of errors to abort upon given the post-selection rule. We define the map from the abort partition to the critical probability under a given decoder  $\Pi : \{\mathcal{P}^{\otimes n}\} \rightarrow \mathbb{R}$ , through  $\Pi[\mathcal{E}_{\text{abort}}] = p_{\text{th}}^c$ . The composition of these maps may be taken to get a map from the post-selection parameter to the conditional logical threshold,  $\Pi[R(c)] = p_{\text{th}}^c$ .

*Optimal post-selection.*—QEC codes can be decoded optimally through MLD, which returns the probabilities of each of the possible logical error cosets. Under the statistical mechanical mapping, this is computed via the disordered partition functions  $Z_E$  for representatives  $E$  of the inequivalent logical error classes. For example, consider a surface code with a single logical qubit, and a measured syndrome  $S$ . There are four inequivalent logical cosets for correction operators  $C$ , which we define as  $\{C_i\}_{i=1,\dots,4}$  such that  $C_i = C_0 L_i$ , where  $C_0$  is a specific correction operator that satisfies the syndrome  $S$ , and  $L_i$  are logical operator representatives that span the inequivalent cosets.

Under MLD of a QEC code, an abort parameter  $c$  can be chosen such that the decoder aborts if  $\max_{E \in \bar{E}(S)} Z_E < c$ , equivalently  $\max_{E \in \bar{E}(S)} \mathbb{P}(\bar{E}) < c$ , where  $\bar{E}(S)$  is the set of errors consistent with the observed syndrome  $S$ . Under MLD, the quenched average of the maximum disordered partition function, e.g.,  $[\max_{\sigma \in \mathcal{P}^{\otimes k}} Z_{\sigma E}]_E$  for a code with  $k$  logical qubits, is the probability of decoding success, as the disordered partition functions correspond to the probabilities of each logical coset.

**Theorem 1.** *Post-selection that aborts if MLD returns a maximum coset probability less than some  $c \in [0, 1]$  is optimal in the following sense. Such post-selection partitions the errors  $\mathcal{E}$  into an abort set  $\mathcal{E}_{\text{abort}}$  of some cardinality  $|\mathcal{E}_{\text{abort}}| = r$ . This partition strictly upper bounds  $\mathbb{P}_{\text{succ}}$  for any abort set with equivalent cardinality  $r$ .*

A proof of Theorem 1 is given in the Supplementary Material.

*Heuristic post-selection.*—As MLD for a general stabilizer code is #P-Complete [28], it remains computationally infeasible to perform optimal post-selection for quantum codes. Inspired by the statistical mechanical mapping and Refs. [10, 13, 16], we propose a heuristic post-selection technique for surface codes. Given the statistical mechanical model of a quantum error correcting code, the non-equilibrium magnetization is  $m := \frac{1}{|S|} \sum_k s_k$ , where the spin degrees of freedom correspond to the stabilizer measurements. This magnetization is a good order parameter for the thermodynamic phases considered in this work, as shown in Ref. [24]. We now define a simple heuristic for post-selection of a surface code via the post selection rule

$$R_{\text{heuristic}}(c) = \{E \mid m(E) < -1 + 2c\}, \quad (3)$$

where  $m(E)$  denotes the non-equilibrium magnetization of the stabilizer measurements given some Pauli error  $E$ . When  $c = 0$ , the set  $\mathcal{E}_{\text{abort}} = \emptyset$  and when  $c = 1$ , the set  $\mathcal{E}_{\text{abort}}$  is the set of errors that produce non-trivial syndromes. This heuristic post-selection rule has the advantage of simplicity over the logical gap rules considered in Refs. [10, 13, 16]. Specifically, the decision of whether to

abort does not require a decoder, but rather only requires the density of stabilizers measuring  $-1$  on the code.

We now apply the statistical mechanical mapping to determine the conditional logical thresholds under the heuristic post-selection rule for surface codes. When  $c = 0$  we never abort, and the statistical mechanical Hamiltonian's behaviour is determined by taking the quenched average over all possible errors  $E \in \mathcal{P}^{\otimes n}$ . Thus, for the toric or surface code with depolarizing noise, we find the disordered eight-vertex model, and the threshold can be approximated numerically as in Ref. [29]. Under MLD, this corresponds to a threshold of  $p_{\text{th}}^{c=0} \approx 18.9\%$  [29]. Under minimum-weight perfect matching (MWPM) decoding, the threshold for this code is instead  $p_{\text{th}}^{c=0} \approx 15.5\%$  [30]. For a pure bit-flip or pure phase-flip channel, such codes are mapped instead to a random-bond Ising model (RBIM) [23], which leads to a MLD threshold of  $p_{\text{th}}^{c=0} \approx 10.94\%$  [31] and a MWPM threshold of  $p_{\text{th}}^{c=0} \approx 10.31\%$  [32].

When  $c = 1$ , we abort whenever the syndrome is non-trivial. In such a case, the accepted errors  $\mathcal{E}_{\text{accept}}$  correspond to the group of logical operators which can be written as the product of stabilizer generators with a chosen set of logical representatives  $\{\prod_k S_k L_m\}$ . The abort partition is the set of errors which produce a non-trivial syndrome. By the symmetry of the statistical mechanical Hamiltonian, we have  $Z_{S_l} = Z_{S_m}$  for all  $S_l, S_m \in \mathcal{S}$ . When the quenched average of the free energy is taken, we note first that above threshold, the free energy cost of a non-trivial logical operator converges to a constant (see Eq. (36) of Ref. [23]). Hence, the non-trivial logical cosets do not contribute to order parameters for this conditional logical threshold, and we may consider only the identity coset. For the identity coset, we have  $Z_{I S_k} = Z_I$  for all stabilizers  $S_k$ , and we note  $Z_I$  corresponds to the non-disordered (or “clean” [25]) Hamiltonian  $H_I$ . For each of the partition functions, the underlying Hamiltonian may be considered equivalent across all disorder parameters, and is given by  $H_I$ .

For the disordered eight-vertex model, with  $E = I$ , the scalar commutators become uniformly  $+1$ , and the Hamiltonian becomes the non-disordered isotropic eight-vertex model. The non-disordered eight-vertex model can be solved exactly to give  $\beta J_c = \frac{1}{4} \log(3)$  [33]. If we substitute this value into the Nishimori conditions, we can rearrange to arrive at  $p_{\text{th}}^{c=1} = 0.5$ , consistent with the numerical estimate in Ref. [10]. While this gives the maximum post-selected conditional logical threshold under MLD, the decoding strategy is simply to do nothing as there are no errors in the accept set, and this is the same for MWPM decoding. Similarly, for a bit-flip or phase-flip channel, the non-disordered Ising model can be solved to give  $\beta J_c = \frac{\log(1+\sqrt{2})}{2}$  [34]. Substituting this into the Nishimori conditions gives  $p_{\text{th}}^{c=1} = \frac{1}{2+\sqrt{2}} \approx 0.2929$ .

For  $0 < c < 1$ , the post-selected conditional logical

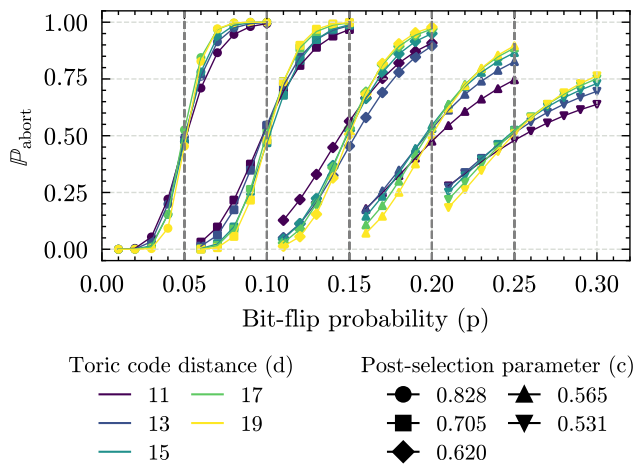


FIG. 1. Abort thresholds of toric codes under bit-flip error channels. Dashed lines indicate analytic predictions using the mean field approximation. Markers indicate numerical results.

threshold lies between the two bounds computed above.

*Abort threshold.*—The existence of an abort threshold is an important necessary condition for post-selected QEC to be scalable. The existence of abort thresholds were first numerically observed in Ref. [10]. Abort thresholds refer to the phenomenon in which in the thermodynamic limit, physical error probabilities above a critical value result in aborting with certainty, while error probabilities below the critical value result in acceptance with certainty. We now show that the abort thresholds of the heuristic post-selection rule can be accurately obtained using a mean field approximation on the spins.

To obtain the mean field approximation, we now compute the expected magnetization in the thermodynamic limit of the spins assuming no inter-spin correlations. For example, consider a toric code under bit-flip noise with probability  $p$ . Each  $\sigma_z$ -type stabilizer has support on four qubits, each of which has a probability  $p$  of suffering a bit-flip. Then, the probability that measuring the stabilizer  $S_k$  returns  $-1$  is  $\mathbb{P}(s_k = -1) = \binom{4}{1}p(1-p)^3 + \binom{4}{3}p^3(1-p)$ , while the probability that it returns  $+1$  is  $\mathbb{P}(s_k = +1) = \binom{4}{0}(1-p)^4 + \binom{4}{2}p^2(1-p)^2 + \binom{4}{4}p^4$ . Then, the expected value of any particular stabilizer's individual magnetization is  $m(p) = \mathbb{E}[m_{s_k}] = -4(p(1-p)^3 + p^3(1-p)) + (1-p)^4 + 6p^2(1-p)^2 + p^4$ .

As each qubit lies in the support of two of each type of stabilizer (e.g., two plaquettes), the probabilities of the spin degrees of freedom are not independent. However, for  $p \ll 1$ , we may approximate the stabilizers as being independent using a mean-field approximation. Under this assumption, in the thermodynamic limit, by the law of large numbers, the total system's magnetization tends towards the expected value given above. If we fix the

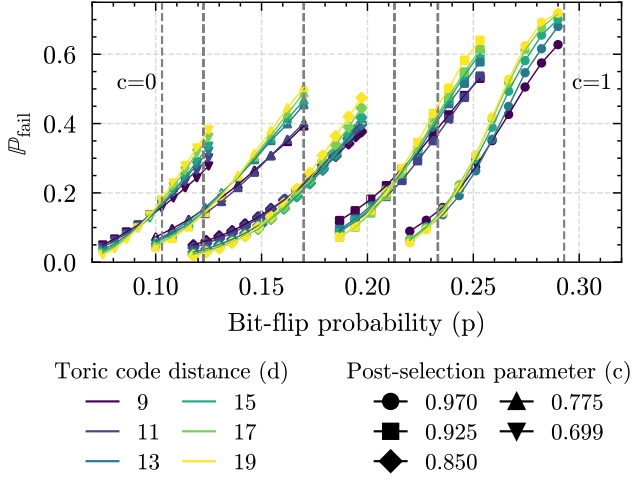


FIG. 2. Conditional post-selected logical thresholds for post-selection parameter  $0.6987 \lesssim c < 1$ . Notation in the plot is similar to Fig. 1.

post-selection parameter  $m_0 = -1 + 2c$ , then in the thermodynamic limit, for  $m(p) < m_0$  we almost surely abort, and for  $m(p) > m_0$ , we almost surely accept, leading to threshold behaviour.

We compute the expected value of the magnetization given bit-flip probabilities of  $p = \{0.05, 0.1, 0.15, 0.2, 0.25\}$ , and sample  $N = 10^7$  errors from these noise channels acting on toric codes of varying sizes, computing abort probabilities given a post-selection parameter equal to the expected magnetization at these probabilities. The results are shown in Fig. 1, demonstrating threshold behaviour near the bit-flip probabilities predicted.

Following the discussion in this section, similar abort thresholds can be computed analytically for any i.i.d. noise model, e.g., depolarizing noise, straightforwardly by computing the expected magnetization. For the optimal post-selection, the abort threshold is fixed at the code's non-post-selected logical threshold.

*Numerical simulations.*—We now investigate the post-selected conditional logical thresholds under our heuristic post-selection rule. We expect that the post-selected conditional logical threshold will increase monotonically with the post-selection parameter  $c$ . We analyze toric codes with parameters  $[[2L^2, 2, L]]$ . We use the Metropolis-Hastings algorithm for a Markov-Chain Monte Carlo (MCMC) method [35] to sample the conditional probability distribution  $\mathbb{P}(E|m(S) > m_0)$ , and we decode the errors using Pymatching [36]. We use the fitting ansatz  $\mathbb{P}_{\text{fail}} = A + Bx + Cx^2$  with  $x = (p - p_{\text{th}})d^{\frac{1}{\nu_0}}$  [37] to extract an estimate of the conditional threshold from the results and indicate the estimate with a dashed line. The results are presented in Fig. 2.

The post-selected conditional logical threshold in-

creases with the post-selection parameter. In other words, as we constrain the non-equilibrium magnetization of the statistical mechanical model more tightly, we increase the phase transition to a higher disorder probability. Moreover, for  $c \lesssim 0.6987$ , the logical threshold of the code is unchanged. This critical value can be determined by the expected magnetization at  $p = p_{\text{th}}^{c=0} \approx 0.103$ . This point arises as a multi-critical point on the phase diagram, which we explain in the next section.

*Thermodynamic phases.*—Through post-selection parameterized by  $c \in [0, 1]$ , we obtain conditional thresholds of  $p_{\text{log,th}}(c)$  and  $p_{\text{abort,th}}(c)$  for the logical error rates and probability of aborting, respectively. Under the heuristic post-selection rule with a bit-flip channel, we expect that the conditional logical thresholds between the two bounds (i.e., at  $c = 0$  and  $c = 1$ ) vary continuously. However, they are difficult to numerically analyze on small-scale code examples, as densities of non-trivial stabilizer measurements on finite codes are discrete and the cardinality of the stabilizers of small code instances of differing sizes generally do not have common factors. Nonetheless, we expect in the thermodynamic limit that clear thresholds emerge.

We plot in Fig. 3 the logical and abort thresholds as a function of the post-selection parameter  $c$ . Under the mean-field approximation, the expected non-equilibrium magnetization possess a  $\mathbb{Z}_2$  symmetry, as it is invariant under the transformation  $p \rightarrow 1 - p$ , and in fact on the domain  $p \in [0, 1]$ ,  $\mathbb{E}[m_{s_k}] \geq 0$ . Moreover, in the thermodynamic limit, for  $c < c_{\text{crit}}$ , where  $c_{\text{crit}} = c \mid \mathbb{E}[m(c)] = p_{\text{th}}^{c=0}$ , we never abort at logical threshold. Because of this, we expect the conditional logical threshold to be unchanged. However, for  $c > c_{\text{crit}}$ , at  $p = p_{\text{th}}^{c=0}$ , we are above the abort threshold, and thus the location of this phase transition can change non-trivially. Thus, in Fig. 3, we find the separation of phases I and IV to be parallel to the x-axis, while the separation of phases II and III to be non-trivial.

We conjecture that the shaded region in Fig. 3 corresponds to useful scalable post-selection. Working in this region is below both abort and logical thresholds, meaning logical failure rates and abort rates can be made arbitrarily small by increasing the code size, but with the advantage that the logical threshold is increased over the non-post-selected case. If a system is above the logical threshold without post-selection, applying post-selection will not bring it below the conditional logical threshold without exceeding the abort threshold. Instead, we emphasise that, although post-selection can increase the logical threshold, the benefits of this increased logical threshold are best harnessed by working with finite-sized codes well below this logical threshold. By assuming a finite-size scaling ansatz of the form  $\mathbb{P}_{\text{fail}} \sim f((p - p_c)d^{\frac{1}{\nu}})$ , post-selection can increase  $p_c$ , thereby shifting the scaling function  $f$  further from criticality [37]. There is also strong numerical evidence that post-selection further im-

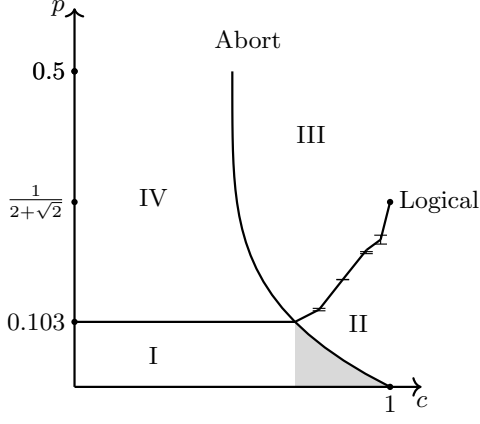


FIG. 3. Phase diagram of toric code under the heuristic post-selection rule with bit-flip error channel. The x-axis represents the post-selection parameter  $c$ . When  $c = 0$ , no post-selection is applied and when  $c = 1$ , we fully post-select, aborting whenever the syndrome is non-trivial. The y-axis represents the i.i.d. bit-flip probability acting on physical qubits. The abort phase boundary is derived using a mean-field approximation of the non-equilibrium magnetization of the spins. The logical phase boundary is trivial for  $c \lesssim 0.6987$  and the multi-critical point can be determined by the expected magnetization at  $p = p_{th}^{c=0}$ . Monte-Carlo simulations are used to estimate the non-trivial boundary. Four thermodynamic phases are identified: I. below abort and logical threshold, II. above abort threshold and below logical threshold, III. above abort and logical threshold, IV. below abort threshold and above logical threshold. The shaded area indicates a regime in which the conditional logical threshold is increased, while remaining below abort threshold. Error bars indicate  $\pm$  one standard deviation of the parameter estimate of threshold probability.

proves the sub-threshold scaling [10]. Our conjecture emphasizes the importance of sub-threshold behavior in finite-sized codes for practical applications, rather than focusing solely on raising the threshold for noisy devices.

*Post-selected QEC in practice.*—We now apply the heuristic post-selection method to open source data reported from experiments where a surface-code memory was initialized on a superconducting processor [26]. An XZZX surface code [38] was initialized with distances 3, 5, and 7. This processor was demonstrated to be below logical threshold, so post-selection can be applied such that the code ends in the shaded region of the phase diagram in Fig. 3. We apply the heuristic post-selection to these results for a single round of error correction. Fig. 4 shows the abort and logical failure probabilities. We observe that for  $c = 0, 0.85, 0.9$ , the data points are below both logical and abort thresholds (Phase I), while for  $c = 0.95$ , they are below logical threshold, but above abort threshold (Phase II). Linear regression was applied to the log-linear plots, followed by hypothesis testing to determine whether the gradient was positive (above threshold) or negative (below threshold). Notably, 6 out

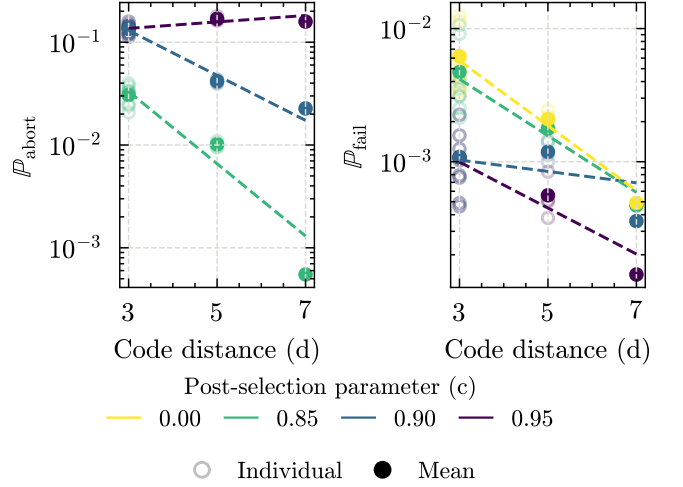


FIG. 4. (Left) Abort probabilities and (right) logical failure probabilities for a single round of error correction on XZZX surface codes initialized on a superconducting quantum computer using the heuristic post-selection [26]. We use the optimized decoding results reported in Ref. [39] that were produced by a neural network decoder with reinforcement learning. We apply the heuristic post-selection rule on this data ex post facto to estimate abort probabilities and conditional logical failure probabilities. Transparent markers indicate individual data of surface codes initialized on different physical qubits. Solid markers indicate averages over all instances of distance  $d$  codes. An exponential curve as a function of  $d$  is fit to each set of data.

of 7 regressions yielded one-sided p-values below 1%, providing statistical evidence for the system's location on the phase diagram. This example demonstrates that our theoretical insights are applicable to experimental implementations of quantum error correction on near-term quantum devices.

*Conclusion.*—Our results point to several promising directions for future work. Our proposed heuristic post-selection technique offers practical advantages without the need for resource-intensive decoding. This, in turn, should facilitate real-time decision-making and reducing computational overhead in post-selected quantum error correction. The post-selected statistical mechanical models we have studied suggest new avenues of research in constrained classical spin models, whereby the ordered-to-disordered phase transition can be deformed with a post-selection parameter. This has potential applications to a very general setting where samples are produced with random disorder and only those passing a post-selection step are kept for further experimentation. A proof or disproof of continuity for the map  $\Pi : [0, 1] \rightarrow [0, 1]$  from the post-selection parameter to the conditional threshold remains an open question. This work can be extended to other noise channels including depolarizing, biased and correlated noise. Finally, circuit-level simulations are desirable to provide more evidence for the applicability of

the heuristic post-selection rule in near-term devices.

*Acknowledgments.*—We thank Samuel Smith and Christopher Chubb for discussions. This work is supported by the Australian Research Council via the Centre of Excellence in Engineered Quantum Systems (EQUS) project number CE170100009, and by the ARO through the QCISS program W911NF-21-1-0007 and IARPA ELQ program W911NF-23-S-0004.

---

\* lucas.english@sydney.edu.au

† Current address: IBM Quantum, IBM Almaden Research Center, San Jose, CA 95120, USA

- [1] A. J. Daley, I. Bloch, C. Kokail, S. Flannigan, N. Pearson, M. Troyer, and P. Zoller, Practical quantum advantage in quantum simulation, *Nature* **607**, 667 (2022).
- [2] S. Bravyi, D. Gosset, and R. König, Quantum advantage with shallow circuits, *Science* **362**, 308 (2018).
- [3] Z. Cai, R. Babbush, S. C. Benjamin, S. Endo, W. J. Huggins, Y. Li, J. R. McClean, and T. E. O’Brien, Quantum error mitigation, *Rev. Mod. Phys.* **95**, 045005 (2023).
- [4] E. T. Campbell, B. M. Terhal, and C. Vuillot, Roads towards fault-tolerant universal quantum computation, *Nature* **549**, 172 (2017).
- [5] M. E. Beverland, P. Murali, M. Troyer, K. M. Svore, T. Hoefler, V. Kliuchnikov, G. H. Low, M. Soeken, A. Sundaram, and A. Vashchillo, Assessing requirements to scale to practical quantum advantage (2022), arXiv:2211.07629 [quant-ph].
- [6] C. Gidney, N. Shutty, and C. Jones, Magic state cultivation: growing T states as cheap as CNOT gates (2024), arXiv:2409.17595 [quant-ph].
- [7] S. Bravyi, A. W. Cross, J. M. Gambetta, D. Maslov, P. Rall, and T. J. Yoder, High-threshold and low-overhead fault-tolerant quantum memory, *Nature* **627**, 778 (2024).
- [8] B. M. Terhal, Quantum error correction for quantum memories, *Rev. Mod. Phys.* **87**, 307 (2015).
- [9] N. Meister, C. A. Pattison, and J. Preskill, Efficient soft-output decoders for the surface code (2024), arXiv:2405.07433 [quant-ph].
- [10] S. C. Smith, B. J. Brown, and S. D. Bartlett, Mitigating errors in logical qubits (2024), arXiv:2405.03766 [quant-ph].
- [11] E. H. Chen, T. J. Yoder, Y. Kim, N. Sundaresan, S. Srinivasan, M. Li, A. D. Córcoles, A. W. Cross, and M. Takita, Calibrated decoders for experimental quantum error correction, *Phys. Rev. Lett.* **128**, 110504 (2022).
- [12] P. Prabhu and B. W. Reichardt, Distance-four quantum codes with combined postselection and error correction, *Phys. Rev. A* **110**, 012419 (2024).
- [13] H. Bombín, M. Pant, S. Roberts, and K. I. Seetharam, Fault-tolerant postselection for low-overhead magic state preparation, *PRX Quantum* **5**, 010302 (2024).
- [14] P. Aliferis, D. Gottesman, and J. Preskill, Accuracy threshold for postselected quantum computation (2007), arXiv:quant-ph/0703264 [quant-ph].
- [15] E. Knill, Quantum computing with realistically noisy devices, *Nature* **434**, 39 (2005).
- [16] C. Gidney, M. Newman, P. Brooks, and C. Jones, Yoked surface codes (2023), arXiv:2312.04522 [quant-ph].
- [17] R. Harper and S. T. Flammia, Fault-tolerant logical gates in the IBM Quantum Experience, *Phys. Rev. Lett.* **122**, 080504 (2019).
- [18] N. Sundaresan, T. J. Yoder, Y. Kim, M. Li, E. H. Chen, G. Harper, T. Thorbeck, A. W. Cross, A. D. Córcoles, and M. Takita, Demonstrating multi-round subsystem quantum error correction using matching and maximum likelihood decoders, *Nat. Commun.* **14**, 2852 (2023).
- [19] L. Postler, S. Heußen, I. Pogorelov, M. Risppler, T. Feldker, M. Meth, C. D. Marciniak, R. Stricker, M. Ringbauer, R. Blatt, P. Schindler, M. Müller, and T. Monz, Demonstration of fault-tolerant universal quantum gate operations, *Nature* **605**, 675 (2022).
- [20] D. Bluvstein, S. J. Evered, A. A. Geim, S. H. Li, H. Zhou, T. Manovitz, S. Ebadi, M. Cain, M. Kalinowski, D. Hangleiter, J. P. Bonilla Ataides, N. Maskara, I. Cong, X. Gao, P. Sales Rodriguez, T. Karolyshyn, G. Semeghini, M. J. Gullans, M. Greiner, V. Vuletić, and M. D. Lukin, Logical quantum processor based on reconfigurable atom arrays, *Nature* **626**, 58 (2024).
- [21] Y. Ye, T. He, H.-L. Huang, Z. Wei, Y. Zhang, Y. Zhao, D. Wu, Q. Zhu, H. Guan, S. Cao, F. Chen, T.-H. Chung, H. Deng, D. Fan, M. Gong, C. Guo, S. Guo, L. Han, N. Li, S. Li, Y. Li, F. Liang, J. Lin, H. Qian, H. Rong, H. Su, S. Wang, Y. Wu, Y. Xu, C. Ying, J. Yu, C. Zha, K. Zhang, Y.-H. Huo, C.-Y. Lu, C.-Z. Peng, X. Zhu, and J.-W. Pan, Logical magic state preparation with fidelity beyond the distillation threshold on a superconducting quantum processor, *Phys. Rev. Lett.* **131**, 210603 (2023).
- [22] R. S. Gupta, N. Sundaresan, T. Alexander, C. J. Wood, S. T. Merkel, M. B. Healy, M. Hillenbrand, T. Jochym-O’Connor, J. R. Wootton, T. J. Yoder, A. W. Cross, M. Takita, and B. J. Brown, Encoding a magic state with beyond break-even fidelity, *Nature* **625**, 259 (2024).
- [23] E. Dennis, A. Kitaev, A. Landahl, and J. Preskill, Topological quantum memory, *J. Math. Phys.* **43**, 4452 (2002).
- [24] C. T. Chubb and S. T. Flammia, Statistical mechanical models for quantum codes with correlated noise, *Ann. Inst. Henri Poincaré Comb. Phys. Interact.* **8**, 269 (2021).
- [25] Y. Li, N. O’Dea, and V. Khemani, Perturbative stability and error correction thresholds of quantum codes (2024), arXiv:2406.15757 [quant-ph].
- [26] R. Acharya, L. Aghababaie-Beni, I. Aleiner, T. I. Andersen, M. Ansmann, F. Arute, K. Arya, A. Asfaw, N. As-trakhantsev, J. Atalaya, R. Babbush, D. Bacon, B. Ballard, J. C. Bardin, J. Bausch, A. Bengtsson, A. Bilmes, S. Blackwell, S. Boixo, G. Bortoli, A. Bourassa, J. Bovaird, L. Brill, M. Broughton, D. A. Browne, B. Buchea, B. B. Buckley, D. A. Buell, T. Burger, B. Burkett, N. Bushnell, A. Cabrera, J. Campero, H.-S. Chang, Y. Chen, Z. Chen, B. Chiaro, D. Chik, C. Chou, J. Claes, A. Y. Cleland, J. Cogan, R. Collins, P. Conner, W. Courtney, A. L. Crook, B. Curtin, S. Das, A. Davies, L. D. Lorenzo, D. M. Debroy, S. Demura, M. Devoret, A. D. Paolo, P. Donohoe, I. Drozdov, A. Dunsworth, C. Earle, T. Edlich, A. Eickbusch, A. M. Elbag, M. El-zouka, C. Erickson, L. Faoro, E. Farhi, V. S. Ferreira, L. F. Burgos, E. Forati, A. G. Fowler, B. Foxen, S. Gan-jam, G. Garcia, R. Gasca, Élie Genois, W. Jiang, C. Gidney, D. Gilboa, R. Gosula, A. G. Dau, D. Graumann, A. Greene, J. A. Gross, S. Habegger, J. Hall, M. C. Hamilton, M. Hansen, M. P. Harrigan, S. D. Harrington, F. J. H. Heras, S. Heslin, P. Heu, O. Higgott, G. Hill,



- J. Hilton, G. Holland, S. Hong, H.-Y. Huang, A. Huff, W. J. Huggins, L. B. Ioffe, S. V. Isakov, J. Iveland, E. Jeffrey, Z. Jiang, C. Jones, S. Jordan, C. Joshi, P. Juhas, D. Kafri, H. Kang, A. H. Karamlou, K. Kechedzhi, J. Kelly, T. Khaira, T. Khattar, M. Khezri, S. Kim, P. V. Klimov, A. R. Klotz, B. Kobrin, P. Kohli, A. N. Korotkov, F. Kostritsa, R. Kothari, B. Kozlovskii, J. M. Kreikebaum, V. D. Kurilovich, N. Lacroix, D. Landhuis, T. Lange-Dei, B. W. Langley, P. Laptev, K.-M. Lau, L. L. Guevel, J. Ledford, K. Lee, Y. D. Lensky, S. Leon, B. J. Lester, W. Y. Li, Y. Li, A. T. Lill, W. Liu, W. P. Livingston, A. Locharla, E. Lucero, D. Lundahl, A. Lunt, S. Madhuk, F. D. Malone, A. Maloney, S. Mandrá, L. S. Martin, S. Martin, O. Martin, C. Maxfield, J. R. McClean, M. McEwen, S. Meeks, A. Megrant, X. Mi, K. C. Miao, A. Mieszala, R. Molavi, S. Molina, S. Montazeri, A. Morvan, R. Movassagh, W. Mruczkiewicz, O. Naaman, M. Neeley, C. Neill, A. Nersisyan, H. Neven, M. Newman, J. H. Ng, A. Nguyen, M. Nguyen, C.-H. Ni, T. E. O'Brien, W. D. Oliver, A. Opremcak, K. Ottosson, A. Petukhov, A. Pizzuto, J. Platt, R. Potter, O. Pritchard, L. P. Pryadko, C. Quintana, G. Ramachandran, M. J. Reagor, D. M. Rhodes, G. Roberts, E. Rosenberg, E. Rosenfeld, P. Roushan, N. C. Rubin, N. Saei, D. Sank, K. Sankaragomathi, K. J. Satzinger, H. F. Schurkus, C. Schuster, A. W. Senior, M. J. Shearn, A. Shorter, N. Shutty, V. Shvarts, S. Singh, V. Sivak, J. Skruzny, S. Small, V. Smelyanskiy, W. C. Smith, R. D. Somma, S. Springer, G. Sterling, D. Strain, J. Suchard, A. Szasz, A. Szein, D. Thor, A. Torres, M. M. Torunbalci, A. Vaishnav, J. Vargas, S. Vdovichev, G. Vidal, B. Villalonga, C. V. Heidweiller, S. Waltman, S. X. Wang, B. Ware, K. Weber, T. White, K. Wong, B. W. K. Woo, C. Xing, Z. J. Yao, P. Yeh, B. Ying, J. Yoo, N. Yosri, G. Young, A. Zalcman, Y. Zhang, N. Zhu, and N. Zobrist, Quantum error correction below the surface code threshold (2024), arXiv:2408.13687 [quant-ph].
- [27] H. Nishimori, Internal energy, specific heat and correlation function of the bond-random Ising model, Prog. Theor. Phys. **66**, 1169 (1981).
- [28] P. Iyer and D. Poulin, Hardness of decoding quantum stabilizer codes, IEEE Trans. Inf. Theor. **61**, 5209–5223 (2015).
- [29] H. Bombín, R. S. Andrist, M. Ohzeki, H. G. Katzgraber, and M. A. Martin-Delgado, Strong resilience of topological codes to depolarization, Phys. Rev. X **2**, 021004 (2012).
- [30] D. S. Wang, A. G. Fowler, A. M. Stephens, and L. C. L. Hollenberg, Threshold error rates for the toric and surface codes (2009), arXiv:0905.0531 [quant-ph].
- [31] A. Honecker, M. Picco, and P. Pujol, Universality class of the Nishimori point in the 2D  $\pm J$  random-bond Ising model, Phys. Rev. Lett. **87**, 047201 (2001).
- [32] C. Wang, J. Harrington, and J. Preskill, Confinement-Higgs transition in a disordered gauge theory and the accuracy threshold for quantum memory, Ann. Phys. **303**, 31 (2003).
- [33] R. J. Baxter, *Exactly solved models in statistical mechanics* (Academic Press, London, 1982).
- [34] L. Onsager, Crystal statistics. I. A two-dimensional model with an order-disorder transition, Phys. Rev. **65**, 117 (1944).
- [35] W. K. Hastings, Monte Carlo sampling methods using Markov chains and their applications, Biometrika **57**, 97 (1970).
- [36] O. Higgott and C. Gidney, Sparse blossom: correcting a million errors per core second with minimum-weight matching (2023), arXiv:2303.15933 [quant-ph].
- [37] F. H. E. Watson and S. D. Barrett, Logical error rate scaling of the toric code, New J. Phys. **16**, 093045 (2014).
- [38] J. P. Bonilla Ataides, D. K. Tuckett, S. D. Bartlett, S. T. Flammia, and B. J. Brown, The XZZX surface code, Nat. Commun. **12**, 2172 (2021).
- [39] J. Bausch, A. W. Senior, F. J. H. Heras, T. Edlich, A. Davies, M. Newman, C. Jones, K. Satzinger, M. Y. Niu, S. Blackwell, G. Holland, D. Kafri, J. Atalaya, C. Gidney, D. Hassabis, S. Boixo, H. Neven, and P. Kohli, Learning to decode the surface code with a recurrent, transformer-based neural network (2023), arXiv:2310.05900 [quant-ph].
- [40] S. Bravyi, M. Suchara, and A. Vargo, Efficient algorithms for maximum likelihood decoding in the surface code, Phys. Rev. A **90**, 032326 (2014).
- [41] D. K. Tuckett, *Tailoring surface codes: Improvements in quantum error correction with biased noise*, Ph.D. thesis, University of Sydney (2020), (qecsim: <https://github.com/qecsim/qecsim>).

## Appendix A: Recap of Pauli Stabilizer Codes

Quantum error correcting codes are a mapping from a *logical* Hilbert space onto a larger *physical* Hilbert space. The logical degrees of freedom are encoded in a subspace of the physical Hilbert space,  $\mathcal{H}_{\text{log}} \subseteq \mathcal{H}_{\text{phy}}$ . We say a code has parameters  $[[n, k, d]]$  if  $\dim(\mathcal{H}_{\text{phy}}) = 2^n$ ,  $\dim(\mathcal{H}_{\text{log}}) = 2^k$  and  $d = \min\{w(L) \mid L \neq I, L|\psi\rangle \in \mathcal{H}_{\text{log}} \text{ for all } |\psi\rangle \in \mathcal{H}_{\text{log}}\}$ . That is, the distance  $d$  is the smallest Hamming weight of a non-trivial logical operator.

Pauli stabilizer codes rely on the stabilizer formalism, in which we specify the logical subspace as the space stabilized by a group of operators we call the stabilizer group  $S$ . That is,  $s|\psi\rangle = +1|\psi\rangle$  for all  $s \in S$  and all  $|\psi\rangle \in \mathcal{H}_{\text{log}}$ . For Pauli stabilizer codes, elements of the stabilizer group are tensor products of Pauli operators, that is  $s = \sigma_{i_1} \otimes \sigma_{i_2} \otimes \cdots \otimes \sigma_{i_n} \in \mathcal{P}^{\otimes n}$ .

Under i.i.d. Pauli noise channels, the probability distribution of errors  $E \in \mathcal{P}^{\otimes n}$  takes the form

$$\mathbb{P}(E) = \prod_{i=1}^n \mathbb{P}(E_i), \quad (4)$$

that is, the product of the probabilities of Paulis affecting each qubit independently.

## Appendix B: Proof of Theorem 1

**Lemma 2.** *Post-selection which aborts when the posterior confidence under MLD is less than some constant  $c \in [0, 1]$  monotonically increases decoding likelihood with respect to  $c$ .*

*Proof.* We first show that post-selection as above for some  $c \in [0, 1]$  lower bounds the probability of decoding success. Without post-selection we have

$$\mathbb{P}_{\text{succ}} = \sum_E \mathbb{P}(E) \mathbb{P}(\text{succ}|E), \quad (5)$$

where  $\mathbb{P}(\text{succ}|E) = \max_{\sigma \in \mathcal{P}^{\otimes k}} Z_{\sigma E}$ . By post-selecting, we partition the set  $E$  into  $E = E_{\text{abort}} \cup E_{\text{accept}}$ , where the new probabilities over  $E_{\text{accept}}$  are normalized through

$$\mathbb{P}(E \in E_{\text{accept}}) = \frac{\mathbb{P}(E)}{\sum_{E \in E_{\text{accept}}} \mathbb{P}(E)}. \quad (6)$$

Assuming that  $\mathbb{P}(\mathbb{P}(\text{succ}|E) > c) \neq 0$ , the conditional probability of decoding success given a post-selection parameter  $c$  is

$$\mathbb{P}_{\text{succ}}^c = \sum_{E \in E_{\text{accept}}} \mathbb{P}(E) \mathbb{P}(\text{succ}|E), \quad (7)$$

$$\geq \sum_{E \in E_{\text{accept}}} \mathbb{P}(E) c, \quad (8)$$

$$= c \sum_{E \in E_{\text{accept}}} \mathbb{P}(E), \quad (9)$$

$$= c. \quad (10)$$

That is, the probability of decoding success is lower bounded by  $c$ . Note that we can trivially upper bound this probability also through aborting whenever the uncertainty is less than some constant  $c$ . Next, we show that by post-selection with parameter  $c$  increases the probability of decoding success without post-selection. The expectation of  $\mathbb{P}(\text{succ})$  over the entire set of errors  $E = \mathcal{P}^{\otimes n}$  can be expressed using the law of total expectation:

$$\mathbb{E}[\mathbb{P}(\text{succ})] = \overbrace{\mathbb{E}[\mathbb{P}(\text{succ})|\mathbb{P}(\text{succ}) > c]}^{>c} \mathbb{P}(\mathbb{P}(\text{succ}) > c) + \overbrace{\mathbb{E}[\mathbb{P}(\text{succ})|\mathbb{P}(\text{succ}) \leq c]}^{\leq c} \mathbb{P}(\mathbb{P}(\text{succ}) \leq c), \quad (11)$$

$$\leq \mathbb{E}[\mathbb{P}(\text{succ})|\mathbb{P}(\text{succ}) > c]. \quad (12)$$



So  $\mathbb{P}_{\text{succ}} \leq \mathbb{P}_{\text{succ}}^c$  with equality if and only if  $\mathbb{P}(\mathbb{P}(\text{succ} \leq c)) = 0$ , that is, all errors lead to a posterior confidence strictly greater than  $c$ . Finally, we show that by increasing the post-selection, we may increase the probability of decoding success. First we note that for two constants  $c, c \in [0, 1]$  with  $c > c$ ,

$$\{E|\mathbb{P}(\text{succ}|E) > c\} \subseteq \{E|\mathbb{P}(\text{succ}|E) > c\}. \quad (13)$$

As with above, we expand the expectation value of  $\mathbb{P}_{\text{succ}}^c$  through:

$$\mathbb{E}[\mathbb{P}(\text{succ})|\mathbb{P}(\text{succ}) > c] = \mathbb{E}[\mathbb{P}(\text{succ})|\mathbb{P}(\text{succ}) > c]\mathbb{P}(\mathbb{P}(\text{succ}) > c|\mathbb{P}(\text{succ}) > c) \quad (14)$$

$$+ \mathbb{E}[\mathbb{P}(\text{succ})|c < \mathbb{P}(\text{succ}) \leq c]\mathbb{P}(c < \mathbb{P}(\text{succ}) \leq c|\mathbb{P}(\text{succ}) > c) \quad (15)$$

and  $\mathbb{E}[\mathbb{P}(\text{succ})|\mathbb{P}(\text{succ}) > c] > \mathbb{E}[\mathbb{P}(\text{succ})|c < \mathbb{P}(\text{succ}) < c]$ . Therefore,

$$\mathbb{E}[\mathbb{P}(\text{succ})|\mathbb{P}(\text{succ}) > c] \leq \mathbb{E}[\mathbb{P}(\text{succ})|\mathbb{P}(\text{succ}) > c], \quad (16)$$

that is,  $\mathbb{P}_{\text{succ}}^c \leq \mathbb{P}_{\text{succ}}^c$  with equality if and only if  $\mathbb{P}(c < \mathbb{P}(\text{succ}) \leq c|\mathbb{P}(\text{succ}) > c) = 0$ .  $\square$

Now, we use this lemma to prove Theorem 1.

*Proof.* First we note that by virtue of MLD, we can write

$$\mathbb{P}_{\text{succ}} = [\max_{\sigma \in \mathcal{P}^{\otimes k}} Z_{\sigma} E]_{E_{\text{accept}}}. \quad (17)$$

As above, we define  $\{E_{\text{accept}} = E | \max_{\sigma \in \mathcal{P}^{\otimes k}} Z_{\sigma} > c\}$ . Then, for any other choice of post-selection which partitions  $E_{\text{accept}}$  with equivalent cardinality but different elements, at least one element of  $E_{\text{accept}}$  must have  $\max_{\sigma \in \mathcal{P}^{\otimes k}} Z_{\sigma} < c$  strictly. Therefore, by Eq. 17,  $\mathbb{P}_{\text{succ}}$  must be strictly smaller for any other post-selection. Hence, this post-selection is optimal.  $\square$

### Appendix C: Analytic and numerical investigation of fully post-selected logical thresholds

The Hamiltonian of the toric code under a bit-flip error channel is

$$H_E = - \sum_{i,j} (-2K + J[Z, E_{i,j,\leftrightarrow}] s_{i,j}^X s_{i-1,j}^X + J[Z, E_{i,j,\updownarrow}] s_{i,j}^X s_{i,j-1}^X), \quad (18)$$

in which the Nishimori conditions relate the temperature and bit-flip probability through

$$\begin{aligned} K &= \frac{1}{2\beta} \log\left(\frac{1}{p(1-p)}\right), \\ J &= \frac{1}{2\beta} \log\left(\frac{1-p}{p}\right). \end{aligned} \quad (19)$$

The Hamiltonian of the toric code under a depolarizing error channel is

$$\begin{aligned} H_E &= - \sum_{i,j} (-K + J[X, E_{i,j,\leftrightarrow}] s_{i,j}^Z s_{i,j+1}^Z + J[Z, E_{i,j,\updownarrow}] s_{i,j}^Z s_{i+1,j}^Z + J[Z, E_{i,j,\updownarrow}] s_{i,j}^Z s_{i-1,j}^Z \\ &\quad + J[X, E_{i,j,\updownarrow}] s_{i,j}^Z s_{i,j-1}^Z + J[X, E_{i,j,\updownarrow}] s_{i,j}^Z s_{i,j+1}^Z s_{i,j}^Z s_{i-1,j}^Z + J[X, E_{i,j,\updownarrow}] s_{i,j}^Z s_{i+1,j}^Z s_{i,j}^Z s_{i,j-1}^Z), \end{aligned} \quad (20)$$

where the Nishimori conditions are

$$\begin{aligned} \beta K &= \frac{1}{2} \log \frac{27}{p^3(1-p)}, \\ \beta J &= \frac{1}{4} \log \frac{3(1-p)}{p}. \end{aligned} \quad (21)$$

We numerically verify the upper bounds on the conditional logical thresholds for depolarizing and bit-flip channels computed in the main article. To perform MLD, we use a matrix product state (MPS)-based tensor network (TN)

decoder [40] implemented in qecsim [41]. We use full contraction of a TN decoder, computing the coset probabilities of a planar surface code of distance  $d$  when the syndrome is trivial. Thresholds of planar surface codes and toric codes are equivalent, as the thermodynamics are unchanged by the boundaries when  $n \rightarrow \infty$ . In Figs. 5 and 6 we plot the posterior confidence that the identity coset will correct successfully (i.e., that by doing nothing, no error has occurred on the logical qubit) for bit-flip and phase-flip channels, respectively. In this fully post-selected regime, i.e., when  $c = 1$ , the pseudothreshold (or breakeven) of the code is equal to the threshold.

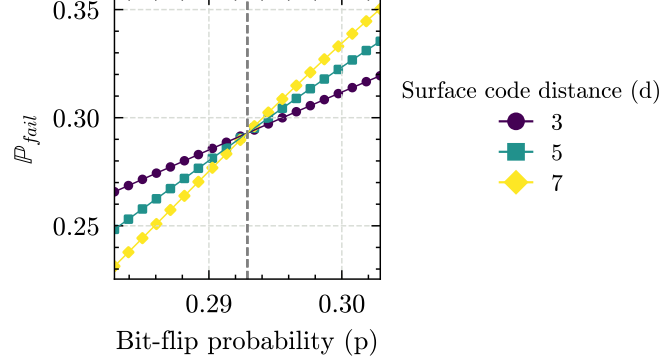


FIG. 5. Probability of decoding failure by doing nothing when syndrome is trivial for a bit-flip channel. The dashed line indicates the theoretical threshold value computed in the main article.

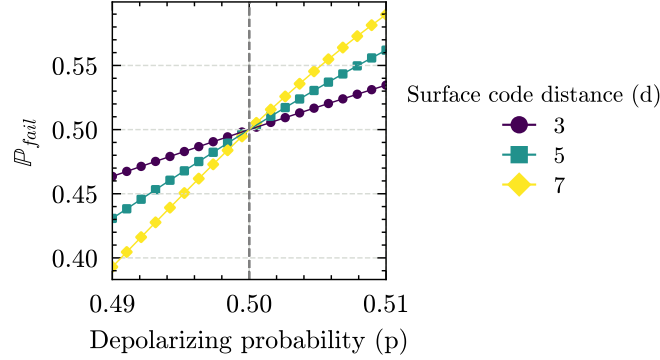


FIG. 6. Probability of decoding failure by doing nothing when syndrome is trivial for a depolarizing channel. The dashed line indicates the theoretical threshold value computed in the main article.

### Abort thresholds under optimal post-selection

Below logical threshold of a code,

$$\lim_{n \rightarrow \infty} \mathbb{P}(\max_E \mathbb{P}(\bar{E}) \geq 1 - \gamma) = 1 \quad \forall \gamma \neq 0, \quad (22)$$

that is, the maximum coset probability approaches 1 almost surely. Similarly, above logical threshold,

$$\lim_{n \rightarrow \infty} \mathbb{P}(\max_E \mathbb{P}(\bar{E}) \leq 1/K - \eta) = 1 \quad \forall \eta \neq 0, \quad (23)$$

that is, the maximum coset probability approaches  $1/K$  (for a logical algebra of dimension  $K$ ) almost surely. Then in the thermodynamic limit, for any  $c \in (1/K, 1)$ , for  $p < p_{\text{th}}$ , we will almost surely never abort, and for  $p > p_{\text{th}}$ , we will almost surely always abort. Therefore, under optimal post-selection, the abort threshold is independent of the post-selection parameter, and fixed at the code's non-post-selected logical threshold.

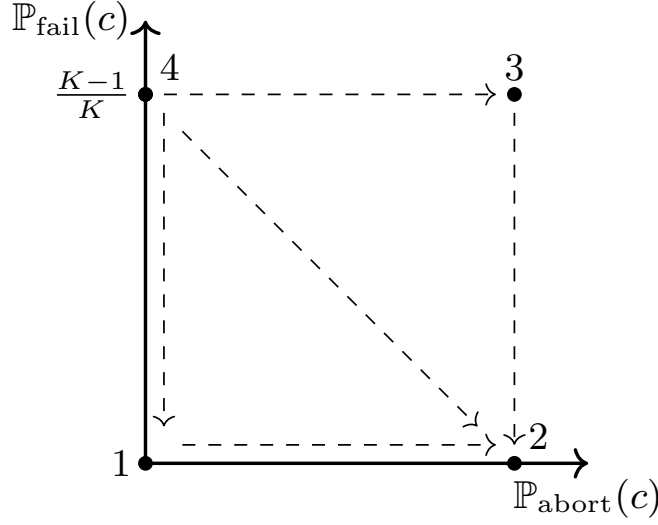


FIG. 7. Probability of conditional failure and probability of aborting in the thermodynamic limit. Four regimes exist which depend on the physical error rates and the post-selection utilized.

#### Appendix D: Details of numerical simulations

If sampling at sufficiently high  $p$  relative to the abort threshold, the probability of aborting tends towards 1, forbidding simple rejection sampling methods. We use the Metropolis-Hastings algorithm for a Markov-Chain Monte Carlo (MCMC) method [35] to sample the conditional probability distribution  $\mathbb{P}(E|m(S) > m)$ , that is probabilities of errors sampled under an i.i.d. bit-flip channel of probability  $p$ , conditioned on the syndrome having magnetization above the post-selection criterion  $m$ . The Metropolis-Hastings algorithm can be used, as the i.i.d. error channels allow the detailed balance condition to be trivially satisfied, and local steps (i.e., flipping single spins) used by such a sampler retains ergodicity, as different logical sectors can be coupled without aborting. Decoding is performed using a minimum-weight perfect matching algorithm through Pymatching [36].

#### Appendix E: Four phases in the thermodynamic limit

Diagrammatically, we can plot in Fig. 7 what the four thermodynamic regimes correspond to in the thermodynamic limit with respect to conditional logical failure probabilities and abort probabilities. These probabilities should be considered such that the probability of failure almost surely approaches 0 or  $\frac{K-1}{K}$  for a logical algebra of dimension  $K$ , and the probability of aborting approaches 0 or 1 almost surely. For example, point 1 corresponds to being below both thresholds, while point 3 corresponds to being above both thresholds. Points 2 and 3 correspond to being above one threshold, while below the other. Dashed lines indicate possible transitions as one increases post-selection. For example, suppose we begin above logical threshold without any post-selection. For  $c < 0.5$ , we are below abort threshold for all  $p \in [0, 1]$ . In this case, we begin at point 4. As we increase post-selection, we move horizontally to the right in the phase diagram, until we possibly become below both thresholds, where we follow the dashed line to point 1. If we increase post-selection further, we may end up above the abort threshold, but below the logical threshold, arriving at point 2. Conversely, we may also begin at a sufficiently high physical error rate, where instead we make the transition from point 4 to point 3 and remain above both thresholds.